Influence of Waveform on Positioning Performance in a TOA/AOA based IR-UWB System

Nammoon Kim, Inho Jeon, Youngok Kim

Department of Electronic Engineering, Kwangwoon University, Korea
kimyoungok@kw.ac.kr

Abstract

The waveform influences on the performance of positioning system based on IR-UWB, but the performance of positioning system under the condition of different waveforms has not studied enough. In this paper, the positioning performance of a hybrid TOA/AOA scheme is evaluated with various waveforms over various IEEE 802. 15. 4a channel models (CMs). Simulation results show that the MHP pulse outperforms other waveforms in CM3 and CM5, and the RRCP outperforms other considered waveforms in CM1 and CM7.

Keywords: *TOA, AOA, IR-UWB, MMSE, MUSIC*

1. Introduction

With the emergence of next-generation location-aware wireless networks and location-based applications such as enhanced 911, U-health service, context aware service, navigation and so on, the importance of location finding technique has been increasingly noticed [1]. In indoor environment, the Time-of-Arrival (TOA) and the Angle-of-Arrival (AOA) techniques are well known schemes for a high precision ranging system. Generally, the TOA based technique show the better accuracy than the AOA technique, because the AOA scheme requires line-of-sight (LOS) wireless communication environment. However, the AOA scheme is more effective than the TOA scheme because it provides two-dimensional (2-D) positioning information with only two base stations (BSs) while the TOA requires minimum three BSs. The proposed hybrid TOA and AOA positioning scheme requires only one BS for 2-D positioning information. The proposed TOA/AOA method can find the location cost effectively compared with the TOA approach that uses 3 BSs.

The TOA based ranging scheme experiences always multipath problem because of its signal's reflection, extinction, and so on. Once a signal passes multipath channels, a BS receives a combined signal that has many different phases [2]. In this case, it is an important part how to find direct path in determining the performance of ranging. The MMSE scheme is employed to estimate channel and to find direct path in the considered TOA scheme, while the MUSIC method is employed to estimate the angle of target mobile terminal in the considered AOA scheme. The performance of proposed scheme is evaluated through the computer simulations over the IEEE 802.15.4a channel models (CMs) [3]. In indoor positioning scheme, if high precision is guaranteed in ranging process, the performance of a hybrid TOA/AOA positioning scheme is highly trustful. Although the short pulse duration of IR-UWB waveform enables to resolve multipath channels accurately, the performance of ranging system under the condition of different waveforms is not studied enough. Since the IR-UWB waveform influences on the performance of

positioning system based on IR-UWB, the positioning performance is evaluated with various waveforms over various channel models in this paper.

2. System Description

A simplified transceiver structure for TOA/AOA based IR-UWB positioning system is shown in Fig. 1. When the known signal is transmitted, the channel impulse response (CIR) can be estimated by applying the inversion or pseudo inversion of the known signal matrix at the receiver. Then, the estimated channel matrix is applied to the TOA estimation process. Each antenna of antenna array receives an emitted signal with different phase, which is caused by distance gap between the transmitter and each receiving antenna, and the angle of target is estimated with the AOA scheme.

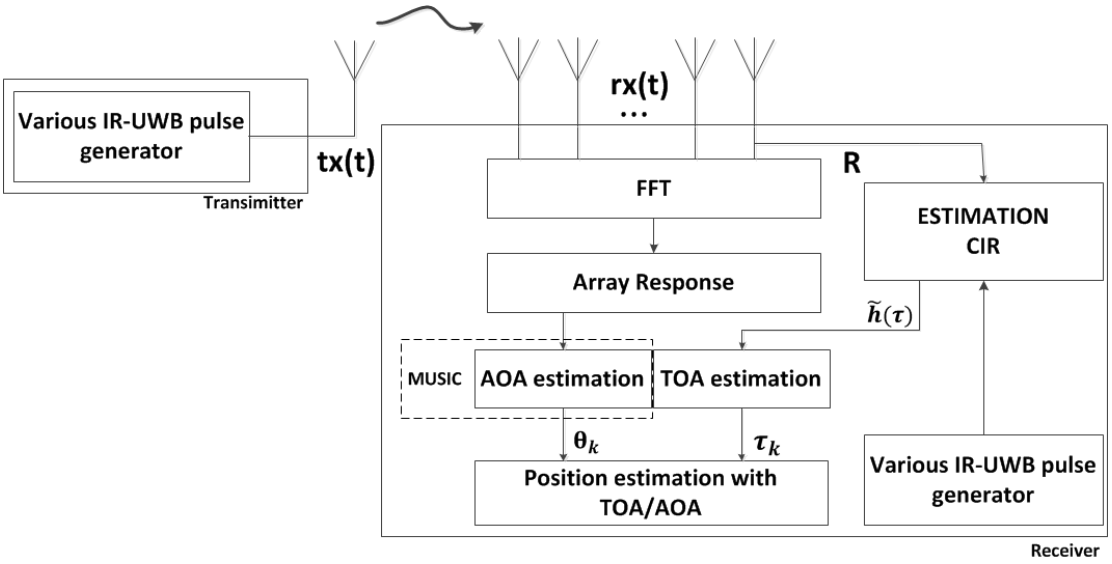

Figure 1. The Hybrid TOA/AOA Positioning System Design

At the receiver, the received signal over the multipath fading channel can be expressed as follows:

$$r(t) = \sum_{k=0}^{L_p-1} a_k s(t-\tau_k) + w(t) \qquad (1)$$

Where L_p is the total number of multipath channels, α_k and τ_k are the amplitude and the propagation delay of the k-th path, respectively. s(·) is the transmitted pulse shape and w(t) is the additive white Gaussian noise with mean zero and variance σ_w^2 . By applying the harmonic signal model, (1) can be represented in frequency domain as follows [4][5]:

$$\begin{aligned} R(f) &= S(f)H(f) + W(f) \\ &= \sum_{k=0}^{Lp-1} \alpha_k S(f) e^{-j2\pi f \tau_k} + W(f), \end{aligned} \qquad (2)$$

The discrete measurement data of (2) can be obtained by sampling at L equally spaced frequencies and is given by

$$R(f) = \sum_{k=0}^{L_p-1} \sum_{l=0}^{L-1} \alpha_k S(m+l) e^{-j2\pi(f_0+l\Delta f)\tau_k} + W(m), \quad (3)$$

where $m = 0, 1, \cdots, M-1$, f_0 is center frequency, and Δf is the sampling interval in frequency domain. Since we use harmonic model in L frequency samples, the N samples are divided into M consecutive segments of length L, where $M = N - L + 1$. Therefore, the transmitted signal S is formed into a $M \times L$ matrix and the sampled signal of (3) can be rewritten as follows:

$$\mathbf{R} = \mathbf{SH} + \mathbf{W} = \mathbf{SVa} + \mathbf{W}, \quad (4)$$

where

$$\mathbf{R} = [R(0) \quad R(1) \quad \cdots \quad R(M-1)]^{\mathrm{T}},$$

$$\mathbf{S} = \begin{bmatrix} S(0) & S(1) & \cdots & S(L-1) \\ S(1) & S(2) & \cdots & S(L) \\ \vdots & \vdots & \ddots & \vdots \\ S(M-1) & S(M) & \cdots & S(M+L-2) \end{bmatrix},$$

$$\mathbf{H} = [H(f_0) \quad H(f_1) \quad \cdots \quad H(f_{L-1})]^{\mathrm{T}},$$

$$\mathbf{W} = [W(0) \quad W(1) \quad \cdots \quad W(M-1)]^{\mathrm{T}},$$

$$\mathbf{V} = [\mathbf{v}(\tau_0) \quad \mathbf{v}(\tau_1) \quad \cdots \quad \mathbf{v}(\tau_{L_p-1})],$$

$$\mathbf{v}(\tau_k) = [1 \quad e^{-j2\pi\Delta f\tau_k} \quad \cdots \quad e^{-j2\pi(L-1)\Delta f\tau_k}]^{\mathrm{T}},$$

$$\mathbf{a} = \left[\alpha_0 e^{-j2\pi f_0\tau_0} \quad \alpha_1 e^{-j2\pi f_0\tau_1} \quad \cdots \quad \alpha_{L_p-1} e^{-j2\pi f_0\tau_{L_p-1}}\right]^{\mathrm{T}}.$$

3. Channel Models and IR-UWB Pulses

3.1. Channel Models

The IEEE 802.15.4a UWB channel models, CM1, CM3, CM5, CM7, are considered. All the channel models are LOS environments. Table 1 shows the characteristics of CMs.

Table 1 Characteristics of Channel Model

Channel model	environment	Distance of from transmitter to receiver
CM1	LOS Residential	7-20m
CM3	LOS Office	3-28m
CM5	LOS Outdoor	5-17m
CM7	LOS Industrial	2-8m

We assumed the direct path has the strongest amplitude among the multipath components because of the LOS effects.

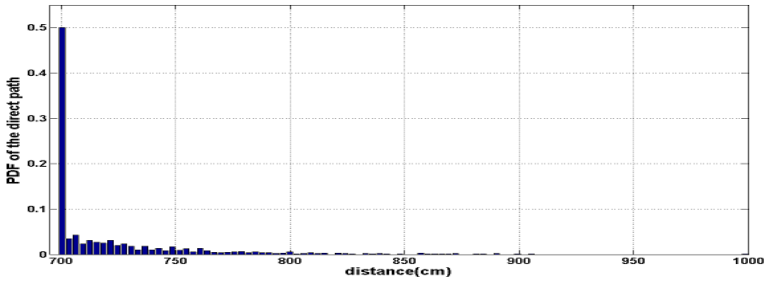

(A) CM1 PDF

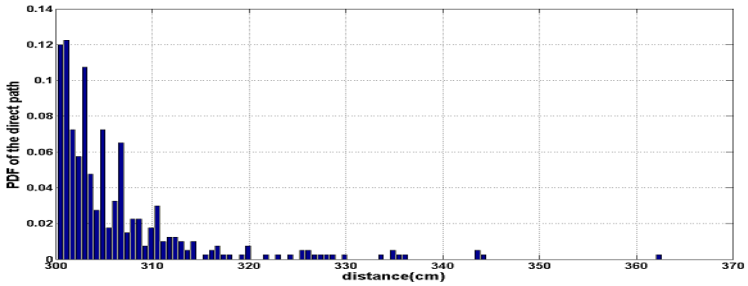

(B) CM3 PDF

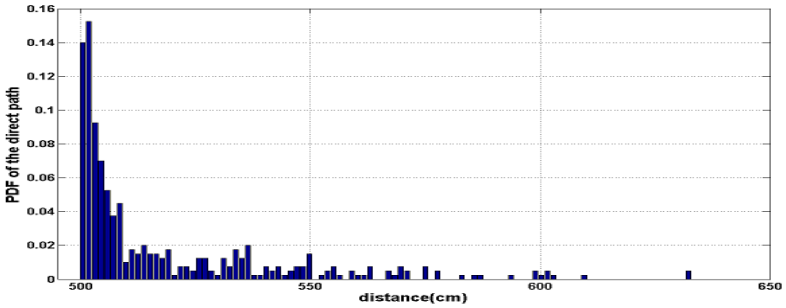

(C) CM5 PDF

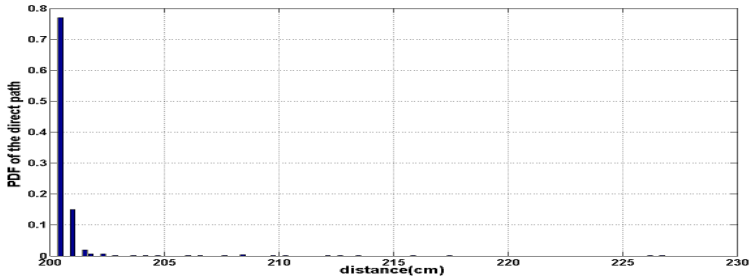

(D) CM7 PDF

Figure 2. PDF According to Channel Model

Fig. 2 shows the distribution of direct path according to channel models. As shown in the figure, the distribution of the direct path is different from the channel models. It indicates that each channel model has different characteristic of direct path and the performance of the proposed system is affected these characteristics of channel model. Therefore, the waveform of best performance is different in the variety of channel models.

3.2. Various IR-UWB Pulses

We employed various IR-UWB pulses for IR-UWB positioning system, such as RRCP, 5th GP, 4th MHP [6], Sine type of PSP [7]. According to the IEEE 802.15.4a standard, the sampling frequency for pulse generation is assumed as 64GHz and the pulse width T_w is 2ns. Fig. 3 shows the time domain representation of RRC, 4th MHP, 5th Gaussian, PS pulse shapes. The RRC pulse is defined as follows:

$$s(t) = \frac{4\beta}{\pi\sqrt{T_p}} \frac{\cos\left[(1-\beta)\pi t/T_p\right] + \frac{\sin\left[(1-\beta)\pi t/T_p\right]}{4\beta(t/T_p)}}{\left(4\beta t/T_p\right)^2 - 1}, \qquad (5)$$

where β is roll-off factor and its value is 0.6, T_p is pulse duration and its value is 2ns. The MHP pulse is fined as follows:

$$s(t) = e^{-\frac{t^2}{4d}}, \qquad (6)$$

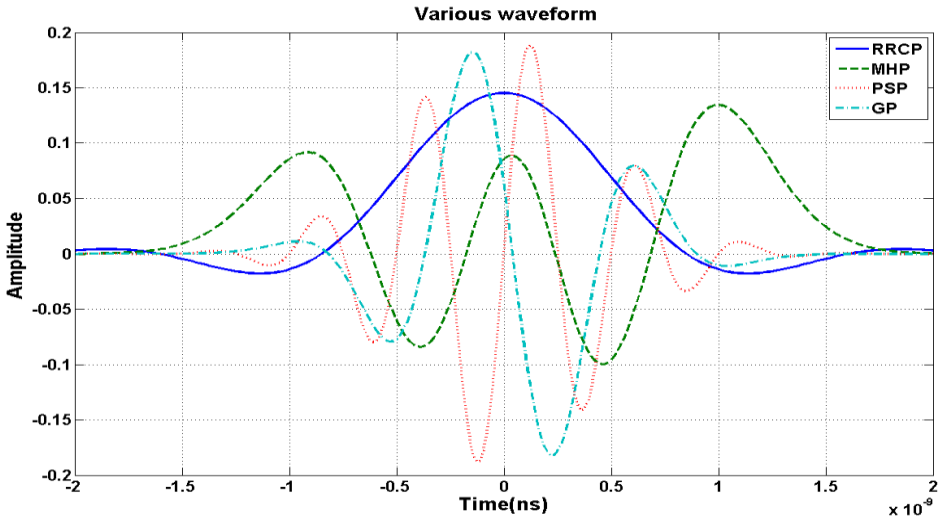

Figure 3. Various IR-UWB Pulses

where d is duration factor and its value is $1/(128 \cdot 10^{17})$. The 4th MHP pulse can be obtained by 4th differentiation of (6). The Gaussian pulse is defined as follows:

$$s(t) = \frac{A}{\sigma\sqrt{2\pi}} e^{-t^2/2\sigma^2}, \qquad (7)$$

The 5th Gaussian pulse can be obtained by 5th differentiation of (7), where the amplitude factor A is 1, the duration factor σ is $300 \cdot 10^{-12}$. The sine type of PS pulse is defined as follows [7]:

$$s(t) = \sin(4\pi 10^9 t)\frac{\sin\left[T\Omega\sqrt{(t/T)^2-1}\right]}{\sinh(T\Omega)\sqrt{(t/T)^2-1}}, \quad (8)$$

where T is duration factor and its value is 10e-9, Ω is bandwidth of frequency domain.

4. Channel Impulse Response Estimation

The CIR can be estimated by applying the inversion or pseudo inversion of the known signal matrix. By multiplying both sides of (4) by the inverse of the signal shape matrix $\mathbf{S}^+$, where $\mathbf{S}^+ = \mathbf{S}^H\{\mathbf{S}\cdot\mathbf{S}^H + (\boldsymbol{\sigma}_w^2)\cdot\mathbf{I}\}^{-1}$ is for MMSE, (4) can be rewritten as follows:

$$\mathbf{S}^+\mathbf{R} = \mathbf{S}^+\mathbf{S}\mathbf{H} + \mathbf{S}^+\mathbf{W} \text{ or } \tilde{\mathbf{H}} = \mathbf{H} + \tilde{\mathbf{W}}, \quad (9)$$

where I represents an identity matrix. Then, the estimated channel matrix $\tilde{\mathbf{H}}$ is applied to the TOA estimation process and the frequency response of the estimated noisy CIR from (9) can be written as follows [4]:

$$H(j2\pi l \triangle f) = \sum_{k=0}^{L_p-1} \alpha_k z_k^l + W_k, \quad (10)$$

where $z_k = e^{-j2\pi\triangle f\tau_k}$ with $\triangle f = 1/L \cdot \triangle t$.

5. AOA Estimation Using MUSIC

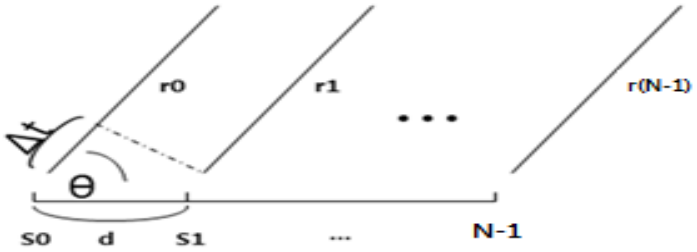

Figure 4. Difference of Detected Signal Depending on Location of Antenna in Array Antennas

The direction of propagation of a radio-frequency wave can be estimated by using the antenna array. Fig. 4 indicates the difference of detected signals depending on the location of an antenna in array antennas. When a transmitted signal arrives to array antennas, each antenna receives the signal with different delays caused from distance gap on each antenna. The received signals between antennas are phase-shifted and they can be defined as follows:

$$e^{-j2\pi f\Delta t} = e^{-j2\pi f d\cos\theta/c} = e^{-j2\pi d\cos\theta/\lambda} = e^{-jkd\cos\theta}\left(k = \frac{2\pi}{\lambda}\right), \quad (11)$$

and the relation of detected signals on S0 and S1 is expressed as follows; $S1 = S0e^{-jkdcos\theta}$. Thus, the detected signals on the array antenna can be defined as steering vector given by [8]:

$$s(\theta) = \left[1 \quad e^{-jkdcos\theta} \quad e^{-2jkdcos\theta} \quad \cdots \quad e^{-j(N-1)kdcos\theta}\right]^T, \tag{12}$$

where N is number of antennas in array.

5.1. MUSIC Algorithm

The MUSIC super-resolution technique is based on eigen-decomposition of the autocorrelation matrix of the received signal vector. The received signal vector can be expressed as follows:

$$R = SH + W, \tag{13}$$

where

$$S = [s(\theta_1)\, s(\theta_2) \quad \cdots \quad s(\theta_M)],$$
$$H = [H_1 H_2 \cdots H_M]^T,$$

and M is number of multi-paths and the matrix S is $N \times M$ matrix.

The autocorrelation matrix of received signal is expressed as follows:

$$R_{RR} = E\{RR^H\} = VAV^H + \sigma_w^2 I = R_s + \sigma_w^2 I, \tag{14}$$

where

$$R_s = VAV^H$$
$$A = \begin{bmatrix} E[|H_1|^2] & 0 & \cdots & 0 \\ 0 & E[|H_2|^2] & \cdots & 0 \\ 0 & 0 & \cdots & E[|H_M|^2] \end{bmatrix}$$

The signal covariance matrix, R_s, is clearly a $N \times N$ matrix with rank M. Therefore, it has N-M eigenvectors corresponding to the zero eigenvalues. Let q_m be such an eigenvector. Then,

$$\begin{aligned} R_s q_m &= SAS^H q_m = 0, \\ &\Rightarrow q_m^H SAS^H q_m = 0, \\ &\Rightarrow S^H q_m = 0 \end{aligned} \tag{15}$$

The last equation of (15) is valid since the matrix A is clearly positive definite. The equation (15) implies that all the N – M eigenvectors (q_m) of R_s corresponding to the zero eigenvalues are orthogonal to all the M signal steering vectors. Let Q_n is the $N \times (N - M)$ matrix of these eigenvectors, then the MUSIC plots the pseudo-spectrum as follows:

$$P_{MUSIC(\theta)} = \frac{1}{\sum_{m=1}^{N-M} |S^H(\theta) q_m|^2} = \frac{1}{s^H(\theta) Q_n Q_n^H s(\theta)} = \frac{1}{|Q_n^H s(\theta)|^2}, \tag{16}$$

Since the eigenvectors making up Q_n are orthogonal to the signal steering vectors, the denominator becomes zero when θ is a signal direction. Therefore, the estimated signal directions are the M largest peaks in the pseudo-spectrum.

6. Simulation Results

In this section, the performances of ranging estimation with TOA scheme and angle estimation with AOA scheme are evaluated with various waveforms. Then, we evaluated the performance of proposed hybrid TOA/AOA based IR-UWB positioning system. As channel models, the CM1, the CM3, the CM5 and the CM7 of IEEE 802.15.4a standard were employed for computer simulations. Simulations are performed with L=120, L_p=57. The center frequency of each channel model was 6GHz (CM1), 4.5GHz (CM3, CM5), 5GHz (CM7), respectively. The number of antennas is 7 and the distance between the antennas d is d=(c/f_c)/2.

6.1. Ranging estimation with TOA scheme

Fig. 5 depicts the ranging estimation error of TOA based IR-UWB system. Each graph represents the result of TOA ranging error according to various pulses. As shown in the figure, all of the results show few centimeters' accuracy. The RRCP outperforms among the considered pulses over all the CMs. The MHP show good performance except for the CM7.

6.2. Angle estimation with AOA scheme

Fig. 6 depicts the angle estimation error of AOA based IR-UWB system. As shown in the figure, all of the results show dozens of degree in all of the CMs. However, the RRCP outperforms than any other pulses in CM1 and CM7, and the MHP shows good performance in CM3 and CM5.

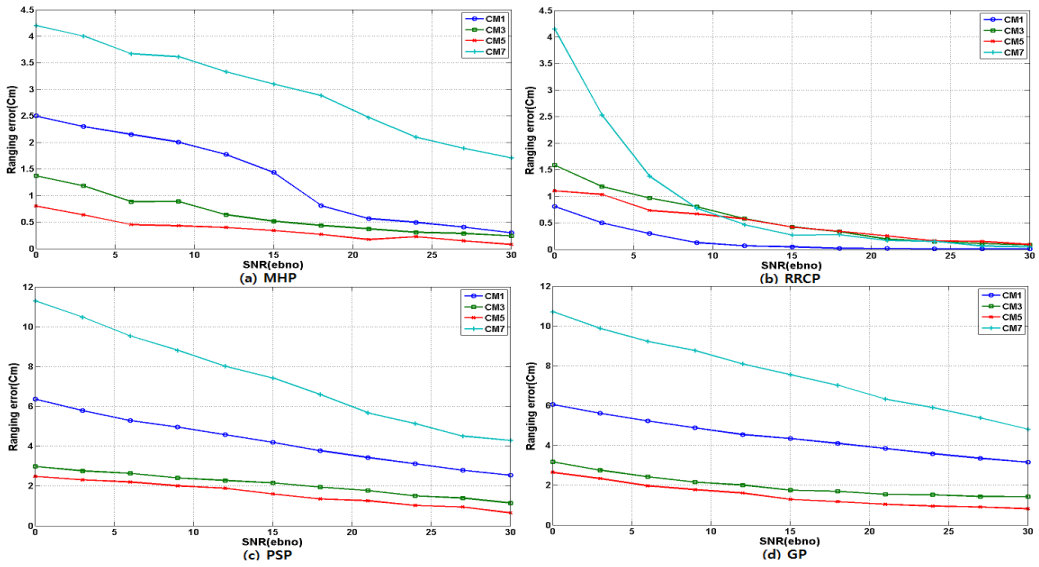

Figure 5. Ranging Estimation Error with Various Waveforms

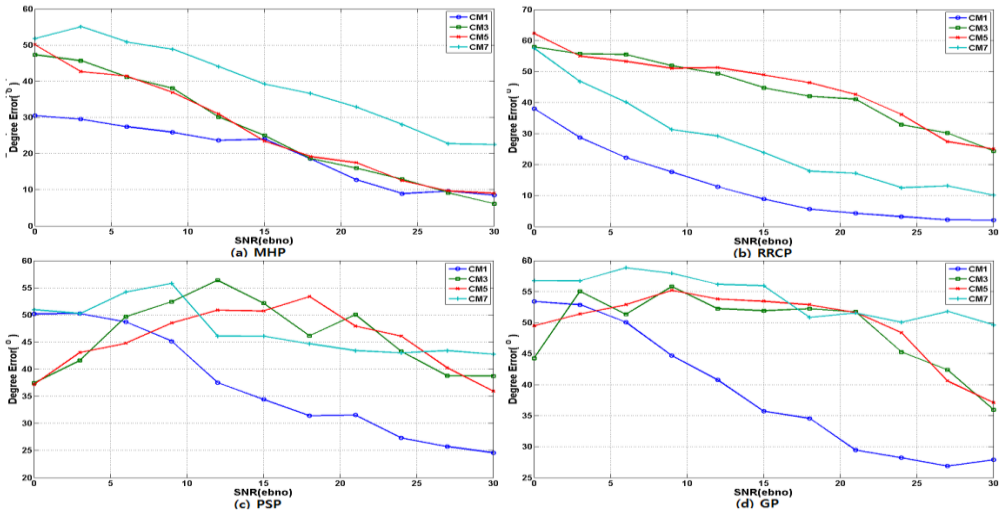

Figure 6. Angle Estimation Error with Various Waveforms

6.3. Hybrid TOA/AOA based IR-UWB positioning scheme

Fig. 7 depicts the positioning estimation error of hybrid TOA/AOA based IR-UWB system. As shown in the figure, the positioning error of CM7 is the smallest in all waveforms. The MHP represents the good performance in the CM1, CM3 and CM5. In the CM7, the RRCP outperforms than other pulses. However, the exact comparison of performance evaluation over the CMs with various waveforms is difficult because the distance from transmitter to receiver is different from CMs. For fair comparison, therefore, it is needed to normalize on distance and the normalized version is shown in Fig. 8.

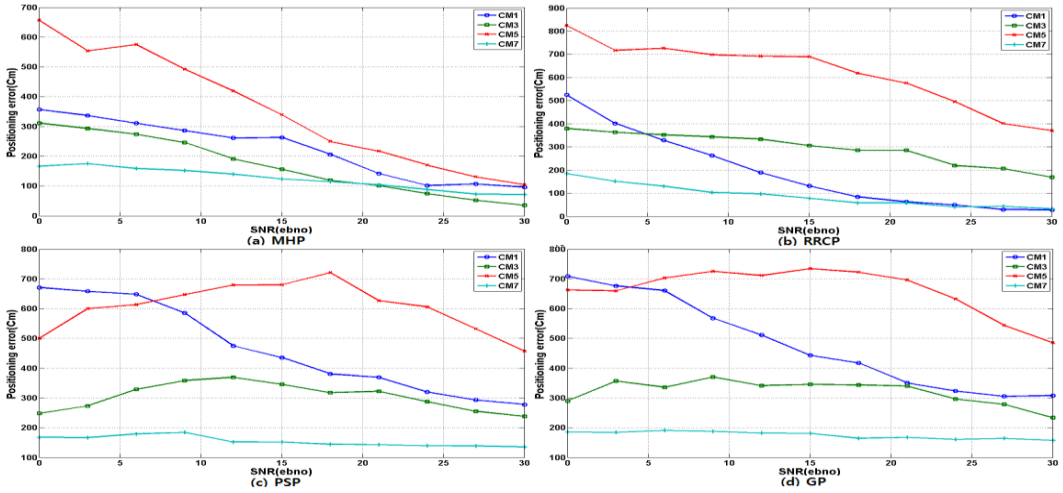

Figure 7. Position Estimation Error of Hybrid Scheme with Various Waveforms

As shown in the figure, the RRCP is a good performance in the CM1 and the CM7, and the MHP is a good performance in the CM3 and the CM5.

6.4. Pulse performance according to CM

Fig. 9 depicts the position estimation error of hybrid TOA/AOA based IR-UWB system according to CMs. As shown in Fig. 9 (a), the MHP outperforms than other pulses when the SNR is lower than 7dB, but the RRCP provides better performance than the MHP when higher than 7dB. In the Fig. 9 (b) and (c), the MHP outperforms than any other pulses in all over the SNR. Fig. 9 (d) shows the RRCP outperforms than other pulses in CM7.

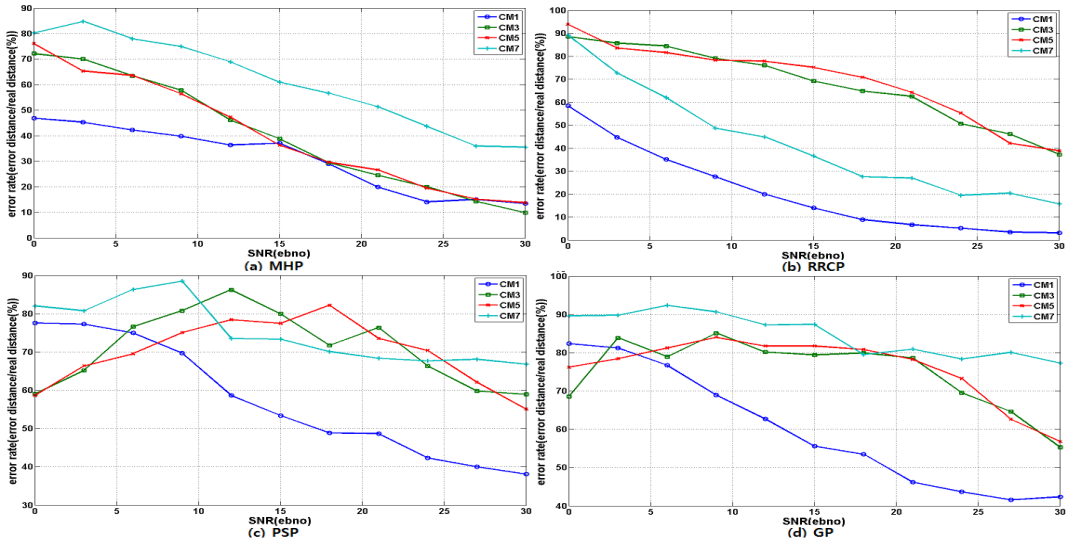

Figure 8. Position Estimation Error with Distance Normalized Version (positioning error/real distance)

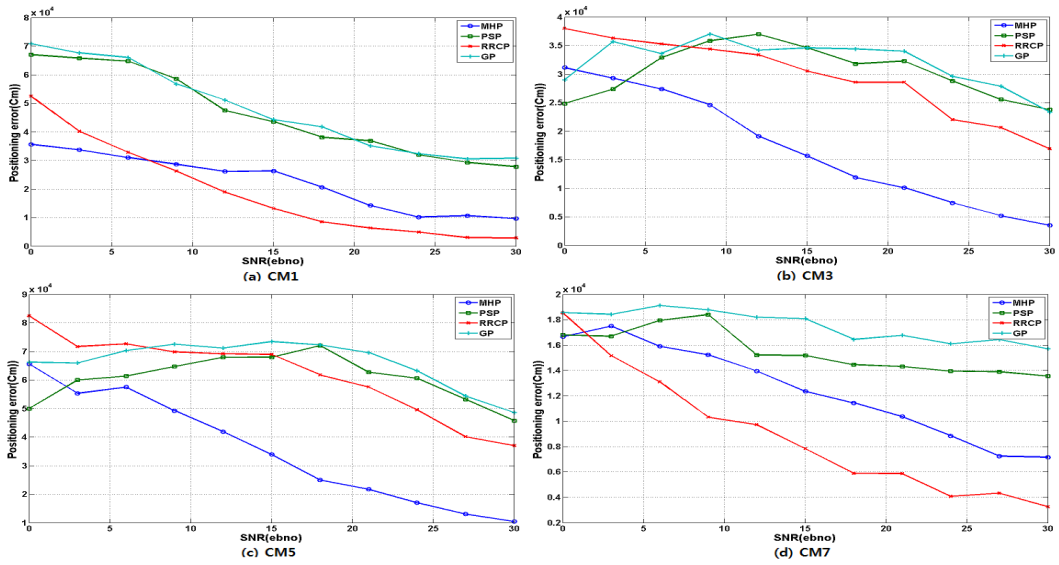

Figure 9. Positioning Estimation Error of Hybrid Scheme with Various Waveform According to Channel Models

7. Conclusion

In this paper, we evaluated performance of hybrid TOA/AOA based IR-UWB positioning system with various shapes of waveforms and CMs. In the TOA, only tiny figurative performance differences were found in the results of system with various pulses, In the AOA, however, the MHP shows good performance in the CM3 and the CM5 and the RRCP shows good performance in the CM1 and the CM7. According to the simulation results, it is observed that the waveform providing good performance is different from the CMs. Generally, the MHP and the RRCP outperforms all the pulses. Although the accuracy of TOA scheme is better than that of hybrid TOA/AOA scheme, the hybrid TOA/AOA based IR-UWB positioning system requires only one BS, unlike the TOA system does three BSs. The hybrid TOA/AOA based IR-UWB positioning system with appropriate pulse depending on the channel environments can be considered for its high performance and economic effects.

Acknowledgment

This research was supported by Basic Science Research Program through the National Research Foundation of Korea (NRF) funded by the Ministry of Education, Science and Technology (No.2010-0008494 and No.2010-0015594).

References

[1] K.pahlavan and P.Krishnamurthy, Principles of Wireless Networks-A Unified Approach. Englewood Cliffs, NJ: prentice-Hall, 2002.

[2] J. D. Taylor, Introduction to Ultra-Wideband Radar Systems, CRC Press, 1995.

[3] IEEE 802.15 WPAN Low Rate Alternative PHY Task Group 4a,"PART 15.4:Wireless MAC and PHY Specifications for LR-WPANs," Draft P802.15.4a/D7, Mar. 2007.

[4] D. Manolakis, V. Ingle, and S. Kogon, Statistical and Adaptive Signal Processing, McGraw-Hill, 2000.

[5] N. Y. Kim, S. Kim, Y. Kim, J. Kang, "A High Precision Ranging Scheme for IEEE802.15.4a Chirp Spread Spectrum System," IEICE Transactions on Communications, E92-B, No. 3, pp. 1057-1061, Mar. 2009.

[6] L. B. Michael, M. Ghavami, and R. Kohno, "Multiple pulse generator for ultra-wideband communication using Hermite polynomial based orthogonal pulses," in Proc. IEEE Conf. UltraWideband Syst. Technol., pp. 47–51, May 2002.

[7] L. Yin, Z. Hongbo, "Interference Mitigation in UWB Communications through Pulse Waveform Design," Environmental Electromagnetics, the 2006 4th Asia-Pacific Conference, pp. 569-572, 1-4 Aug. 2006.

[8] F. B. Gross, "Smart Antennas for Wireless Communications with Matlab," McGraw-Hill, 2005.

Authors

Nammoon Kim received the B.S. degree in electronics engineering from Kwangwoon University, Seoul, Korea in 2011. He is currently working toward the M.S. degree at the Kwangwoon University.

His research interests include ultra-wideband wire-less communication systems, high precision positioning techniques and system.

Inho Jeon received the B.S. degree in electronics engineering from Kwangwoon Uni versity, Seoul, Korea in 2009. He is currently working toward the M.S. degree at the Kwangwoon University.

His research interests include ultra-wideband wire-less communication systems, high precision positioning techniques and system.

Youngok Kim received the B.S. degree in mechanical engineering from Yonsei University, Seoul, Korea in 1999, and the M.S. and PH.D. degrees in electrical and computer engineering from the University of Texas at Austin, Austin, in 2002 and 2006, respectively. From 2006 to 2 008, he was a senior researcher at Infra Laboratory of Korea Telecom (KT), Seoul, Korea. In March 2008, he joined the Department of Electronic Engineering of Kwangwoon University, Seoul, Korea, as an Assistant Professor. His research interests include ultra-wide band wireless communication systems, OFDM-based systems, precise ranging and location systems, PAPR reduction techniques, diversity techniques for wireless systems, and multiple-access schemes in multi-carrier systems.